JOURNAL OF MATERIALS SCIENCE 17 (1982) 3663–3671

Effect of electric fields on solid-state reactions between oxides

Part 4 *Interdiffusion in polycrystalline calcium oxide and silicon dioxide pellets*

I. W. M. BROWN, K. J. D. MACKENZIE
Chemistry Division, DSIR, Private Bag, Petone, New Zealand

Interdiffusion in sintered polycrystalline pellets of CaO and SiO_2 occurs predominantly by migration of Ca into SiO_2 and is influenced by the application of d.c. electric fields which increase the penetration distance when the silica is negatively charged, and markedly decrease the diffusion when the polarity is reversed. Pseudowollastonite (α-$CaSiO_3$) is formed in the interfacial region of the silica pellets under all conditions, with β-Ca_2SiO_4 also appearing in the SiO_2 (–ve) electrolysed samples, possibly as a result of stabilization by the excess Ca present which also occurs as CaO interpenetrating the silica pellet. Diffusion coefficients estimated for both the unelectrolysed and field-assisted (SiO_2–ve) samples are similar to those for Ca diffusion in α-$CaSiO_3$, but samples electrolysed under reverse polarity conditions (SiO_2 + ve) have a much larger diffusion activation energy. The effective electrical mobilities of Ca in the CaO–SiO_2 system derived from these results are discussed.

1. Introduction

In previous parts of this paper [1, 2], it has been established that externally applied d.c. electric fields influence the interdiffusion processes in polycrystalline divalent–trivalent oxide systems such as CaO–Al_2O_3 [1] and MgO–Al_2O_3 [2]. In both these systems, the application of the electric field displaces the measured diffusion profile by an amount which compares reasonably well with that calculated from electrical conductance and diffusion measurements, the calculated values of the effective electrical mobilities being about four times smaller than the measured values in both systems.

Another binary oxide system of considerable practical importance in the cement and refractories industries is CaO–SiO_2. Although subject to similar experimental difficulties to the CaO–Al_2O_3 system, in that a number of product phases of different composition can be formed, it was included in the present series of studies both because of its practical significance and for its interest as a divalent–quadrivalent system. The reaction between CaO and SiO_2 powders has been extensively studied (see, for example, the literature cited by Gebauer and Fitzer [3]). Of the few studies reported on the interaction of monocrystalline or polycrystalline bulk oxides, the electron microprobe investigation by Hayami and Ogura [4] is particularly relevant since it established, by use of platinum markers, that the reaction proceeds by diffusion of Ca into SiO_2 rather than *vice versa*, a result which was subsequently rationalized by Belyaev in terms of differences in the "mean interaction energies" calculated for the two oxides from their heats of formation, dissociation and sublimation [5]. In an electron microprobe study of the reaction of single-crystal CaO with fine-grained silica-gel compacts, and silica-glass slabs with polycrystalline $CaCO_3$, Gebauer and Fitzer [3] deduced that the initial stage of the reaction is characterized by the formation of a substantial amount of a silica-rich phase of composition CS_3–CS_5 at the silica side of the couple, with a smaller amount of CS–C_2S appearing at the CaO side (C = CaO, S = SiO_2). Further reaction resulted in

0022–2461/82/123663–09$03.58/0

the movement of Ca through the product layers with the SiO_2, but some counter-diffusion of Si was also postulated. This work suffers from the serious drawback that markers were not used, and the resulting reaction scheme is also at variance with the commonly accepted sequence originally proposed by Jander and Hoffmann [6] on the basis of powder mixture studies. In that scheme, an intermediate layer of C_2S forms initially, whereupon the product at the silica face becomes gradually Si-rich, passing through the phases C_3S_2 and CS. The product at the CaO face remains relatively Ca-rich (C_3S and C_2S) [6].

The purpose of the present work was to investigate the interdiffusional behaviour of polycrystalline sintered compacts of SiO_2 and CaO both in the presence and absence of an external d.c. electric field. The elemental concentration profiles in the reactant pellets were determined by an EDAX probe in conjunction with a scanning electron microscope and the nature of the various crystalline interfacial phases was investigated by X-ray diffraction using a serial grinding technique [1].

2. Experimental procedure

The oxide starting materials were prepared by separately calcining Analar grade $CaCO_3$ and Baker silicic acid, the latter being chosen from a number of precipitated silicas and silica gels on account of its significantly lower alkali content (0.004% Na, 0.0002% K, determined by flame photometry). Pellets of 10 mm diameter pressed from CaO at 40 MPa and from SiO_2 at 6 MPa were separately sintered in platinum dishes at 1450 to 1500° C for 4 h, the resulting SiO_2 (cristobalite) compacts being 88.4% dense and the CaO pellets being 87.8% dense. Diffusion couples containing 50 S.W.G. (2.5×10^{-5} m diameter) platinum wire markers were heated in a vertical electrolysis cell between platinum foil electrodes in an electric muffle furnace for 72 h at 1250 to 1400° C. The temperature was controlled to better than ± 1° C and was measured by an independent thermocouple located in the electrolysis cell. On attaining the preselected temperature, a d.c. field (typically 1.69×10^5 V m^{-1}) was applied across the electrodes from a Philips PW4022 EHT power supply as previously described [2]; unelectrolysed control experiments were also made at each temperature. After the completion of the heating, the samples were cleaved across the diameter, one portion being prepared for EDAX examination and the other being examined by X-ray diffraction as previously described [2].

3. Results and discussion

3.1. Elemental concentration profiles

Examination of the marker positions after the diffusion anneal in both the electrolysed and unelectrolysed samples confirmed the previous finding [4] of predominantly Ca diffusion into SiO_2; in some higher temperature experiments in which the CaO pellet was negatively charged with respect to SiO_2, a small but finite amount of Si counter-diffusion was also noted. The predominant diffusion of Ca into SiO_2 produces in the latter a band of calcium silicate, the composition of which was examined in detail by X-ray diffraction (XRD, Section 3.2.). However, the existence of this band gave rise to major problems in determining the precise positions of the concentration profiles, since at higher temperatures the product did not adhere to the SiO_2 pellets, but was friable and crumbled to dust as soon as the pellets were separated. This phenomenon (known as "dusting" in cement technology) results from the volume change associated with the inversion of α, α' or β-C_2S to the γ-form on cooling, and made the direct determination of the Ca penetration distance by SEM/EDAX impossible at the two highest temperatures (1350 and 1400° C). In order to overcome this difficulty, an indirect method was used in these cases, in which the powdery reaction product was carefully collected and weighed when the pellets were separated. The thickness of the product layer corresponding to the friable material was then calculated, assuming a density of 2.7 g cm^{-3} for the interfacial material when it was *in situ*. This density was taken as the mean of the measured density of the host SiO_2 pellet (2.15 g cm^{-3}), the bulk structure of which is considered to influence the structure of the product, and the density of β-C_2S (3.28 g cm^{-3} [7]), representing the crystallographic form in which the C_2S was found by XRD to exist in most of the samples not affected by dusting. Fig. 1 shows a set of diffusion profiles for samples annealed at 1300° C, at which temperature the product layer remained intact.

The behaviour shown in Fig. 1 is typical of all temperatures, with slightly enhanced Ca penetration occurring in the SiO_2(−ve) samples, the penetration being markedly retarded for

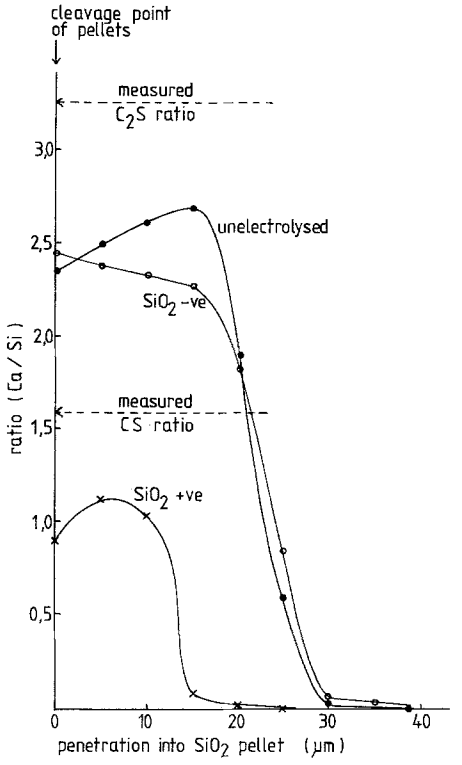

Figure 1 Diffusion profiles of Ca in the silica pellet of electrolysed and unelectrolysed CaO/SiO_2 couples. Annealing time 72 h, temperature 1300° C, mean electric field strength 1.69×10^5 V m^{-1}.

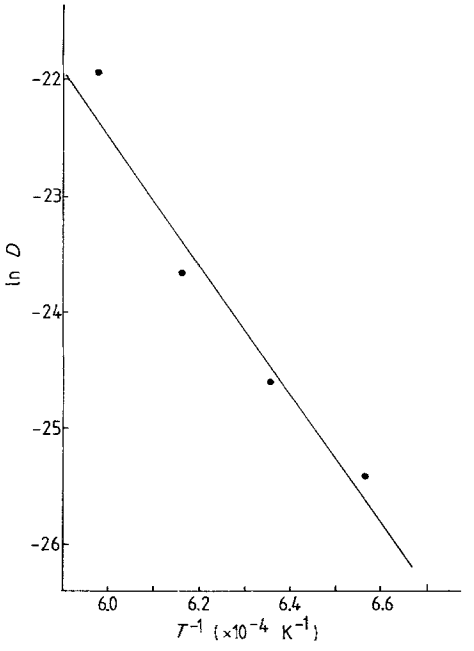

Figure 2 Temperature dependence of Ca diffusion coefficient in the silica pellet of unelectrolysed CaO/SiO_2 couples. Annealing time 72 h.

SiO_2 (+ ve). This result is again consistent with the predominant migration of Ca into SiO_2. EDAX measurements of the Ca/Si ratios in synthetic C_2S and CS are also indicated in Fig. 1, showing that the composition of the interfacial reaction product lies between CS and C_2S in the unelectrolysed and SiO_2(−ve) samples, whereas in the SiO_2(+ ve) samples in which Ca migration is retarded, the interfacial composition is closer to CS.

Diffusion coefficients for the migration of Ca into SiO_2 under applied-field and zero-field conditions were deduced from the SEM/EDAX concentration profiles, following a similar procedure to that previously used in the $MgO-Al_2O_3$ system [2]. As in that work, the diffusion was assumed to proceed into a semi-infinite solid with constant surface composition. The resulting diffusion coefficients are plotted as a function of temperature for zero-field conditions in Fig. 2, and for the two electrolysis conditions in Fig. 3.

In view of the corrections for the effects of dusting which had to be applied to the diffusion profiles at the two highest temperatures, the scatter of the experimental points about the regression lines shown in Figs 2 and 3 is satisfactory, the regression coefficients being 0.944, 0.959 and 0.999 for the zero field, SiO_2(− ve) and SiO_2(+ ve) cases, respectively. The linear regression analyses yield activation energies of 109.9 kcal mol^{-1} for zero-field conditions, the complete expression for the temperature dependence of the diffusion coefficient being

$$D_{(\text{unelec})} = 4.29 \times 10^4 \times \exp(-109\,900/RT)\ \text{cm}^2\ \text{sec}^{-1}. \quad (1)$$

A similar magnitude of activation energy is calculated for the SiO_2(− ve) case (98.7 kcal mol^{-1}), in which the complete diffusion expression is

$$D_{(SiO_2\text{-ve})} = 1.62 \times 10^3 \exp(-98\,700/RT)\ \text{cm}^2\ \text{sec}^{-1}. \quad (2)$$

but for the SiO_2(+ ve) case, the activation energy is much greater (202.3 kcal mol^{-1}), the complete expression being

$$D_{(SiO_2\text{+ ve})} = 7.84 \times 10^{16} \times \exp(-202\,300/RT)\ \text{cm}^2\ \text{sec}^{-1}. \quad (3)$$

In the $MgO-Al_2O_3$ system [2], a marked difference was also observed between the activation

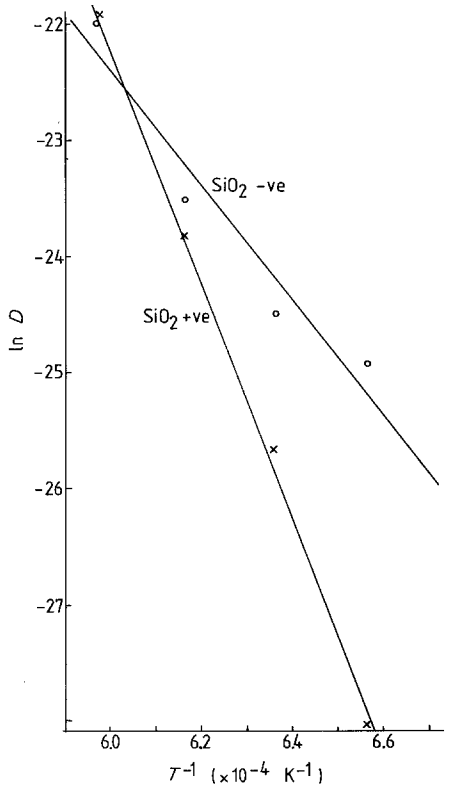

Figure 3 Temperature dependence of Ca diffusion coefficient in the silica pellet of electrolysed CaO/SiO_2 couples. Annealing time 72 h, mean electric field strength 1.69×10^5 V m^{-1}.

energies for field-assisted and field-hindered diffusion; in that system, however, the lower activation energy (which also coincided with the energy for zero-field diffusion) was found for the field-hindered case, by contrast with the present result. Reasons for the different behaviour of the two systems are not immediately obvious.

Comparison of the present activation energies with reported self-diffusion energies shows that the zero-field and SiO_2 (− ve) values are smaller than that reported for self-diffusion of Si in SiO_2 (138.4 kcal mol^{-1}) [8], but larger than the energies reported by various authors for Ca in CaO which range from 28 to 81 kcal mol^{-1} [9], the higher value corresponding to a polycrystalline compact annealed in air. However, the present activation energies are closer to that reported for Ca diffusion in α-CS (112 kcal mol^{-1}) [10]. The pre-exponential factor for this diffusion (7.0×10^4 cm^2 sec^{-1}) is also similar to those found here for the zero-field and SiO_2 (− ve) situations, suggesting that under these conditions the movement of Ca into SiO_2 is determined by its ability to traverse the intervening band of calcium silicate reaction product. This suggestion is supported by the X-ray identification of α-CS as a major interfacial product in all samples (Section 3.2.).

The extremely high activation energy found for the field-hindered experiments does not correspond with the energy of any reported process in CaO–SiO_2, and probably reflects significantly increased difficulty experienced by Ca^{2+} in migrating against the field.

3.2. X-ray phase profiles in the reacted pellets

X-ray diffraction of the pellet reaction zones showed the principal reaction products to be α′ and β-C_2S and α-CS. No C_3S was found in any of the samples, but in the SiO_2 (− ve) samples where high concentrations of Ca were electrolysed into the silica pellet, the Ca in excess of that required for CS and C_2S formation occurred as interstitial CaO at all temperatures but 1400° C. The absence of CaO in the silica pellets at 1400° C may be due to the incipient formation of some C_3S at this temperature, but, if so, its concentration or crystallinity is insufficient for detection by X-ray diffraction.

Figs 4 and 5 show the profiles of the silica polymorphs and α-CS (pseudowollastonite) occurring in the silica pellets at 1300° C. Although several silicate phases other than α-CS were also found under various conditions of temperature and electrolysis, only α-CS is plotted in Fig. 5, since this was the only silicate phase found in all samples. The trends shown in Figs 4 and 5 are typical for all samples, but some individual differences were noted in the phase compositions at different temperatures. These are discussed below.

3.2.1. Tridymite

This phase occurred in the reaction zone of the silica pellet only in the silica (+ ve) experiments at 1250, 1300 and 1350° C. The formation of this silica polymorph requires the presence of foreign ions (usually Na^+) which stabilize the structure. Since it is formed only when the CaO pellet is negatively charged (SiO_2 + ve), the mechanism of its formation probably involves the electrolysis of such impurity sodium ions as occur in the silica towards the interface. This process might also help to explain the tridymite concentration "waves" noted in all samples containing this phase (Fig. 4),

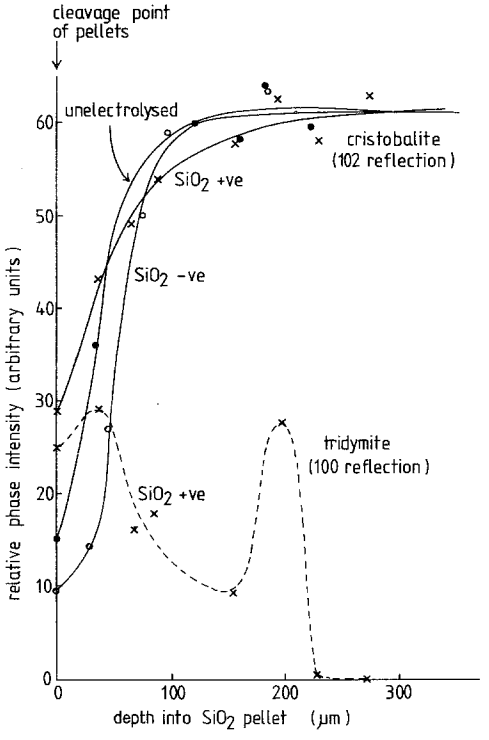

Figure 4 X-ray concentration profiles of silica polymorphs in the silica pellet of electrolysed and unelectrolysed CaO/SiO_2 couples. Annealing time 72 h, temperature 1300° C, mean electric field strength 1.69×10^5 V m^{-1}.

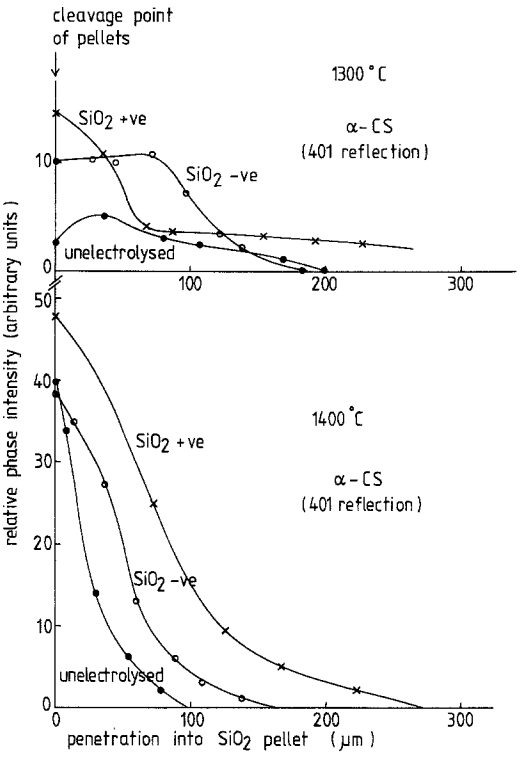

Figure 5 X-ray concentration profiles of α-CS (pseudo-wollastonite) in electrolysed and unelectrolysed CaO/SiO_2 couples. Annealing time 72 h, mean electric field strength 1.69×10^5 V m^{-1}.

which was, however, extremely susceptible to orientation effects, showing marked but random differences in the intensity behaviour of several of the major tridymite X-ray reflections throughout the reaction zone. For this reason, detailed conclusions cannot be drawn from the profile of this phase, although its presence in the interfacial region of the SiO_2 (+ ve) samples is clearly demonstrated.

3.2.2. Dicalcium silicate

In all the field-assisted samples (SiO_2 − ve), this phase occurred as the β-polymorph, presumably stabilized by the additional Ca available under these conditions. As already noted, the conditions favouring β-C_2S formation also give rise to free CaO within the silica pellet, but because of the coincidence of the major CaO X-ray peak with a β-C_2S peak the inter-relationship of these two phases is difficult to quantify. The concentration of β-C_2S, estimated semi-quantitatively from its X-ray intensities, was greatest at the lowest temperature and progressively decreased with increasing temperature. In samples fired at 1400° C it was not found at all, having apparently completely inverted on cooling to the γ-form which, due to its friability, gave rise to the problems discussed in Section 3.1. The identity of the friable product was confirmed as solely γ-C_2S by X-ray diffraction.

No polymorph of C_2S was found in any samples electrolysed under field-hindered conditions (SiO_2 + ve), but in the zero-field samples at the two lowest temperatures, some α′-C_2S was detected. Since this is one of the high-temperature forms which on cooling to ~ 650° C normally inverts to the β-form [11], its appearance in these samples is unexpected. Alkali metals are known to stabilize this phase [11], and one possible explanation is that the small impurity concentration of Na^+ and K^+ present in the silica pellets is sufficient to stabilize α′-C_2S under zero-field conditions. Under SiO_2 (− ve) conditions, the alkali metal ions will be electrolysed away from the reaction zone, while in the SiO_2 (+ ve) experiments, although the alkali metal concentration in the reaction zone is increased (evidence for this is the formation of tridymite), the Ca concentration in the reaction zone is too depleted under these conditions for C_2S of any type to be formed.

3.2.3. Monocalcium silicate

The concentration profiles of pseudowollastonite (α-CS) are shown in Fig. 5. By contrast with β-C_2S, the concentration and degree of penetration of this phase into the silica pellets increases with increasing temperature, being particularly in evidence at 1400° C (Fig. 5). At all temperatures, the degree of penetration was greatest in the SiO_2(+ ve) experiments, with less penetration occurring in the SiO_2(− ve) experiments. This apparently contrary behaviour can be understood by taking into account the occurrence of the other silicate phases; in the SiO_2(+ ve) case, CS is the only silicate phase formed, whereas in the SiO_2(− ve) and zero-field samples, C_2S also occurs. Likewise, the increased concentrations of CS with increasing temperature may be related to the competitive formation of C_2S, which *decreases* with increasing temperature.

X-ray analysis of the CaO pellets after reaction showed evidence of α'-C_2S formation in the surface regions of the SiO_2(+ ve) samples, but the penetration depth was negligible. X-ray diffraction also indicated a 0.05 to 0.1 mm thick band in the CaO pellets immediately adjacent to the interface, in which the relative intensities of the CaO reflections were extremely variable, and not consistent with the intensity ratios of well-characterized CaO. This suggests that the CaO structure in this region is perturbed, probably as a result of Ca^{2+} depletion by its migration into the silica pellet, with limited compensating counter-diffusion. Additional support for this explanation is found in the fact that the effect was strongest where Ca migration was facilitated (SiO_2–ve), and increased with increasing temperature.

Comment is necessary regarding the discrepancy between the Ca penetration distances inferred from X-ray measurements (Figs 4 and 5) and those measured by SEM/EDAX, which are up to an order of magnitude smaller (Fig. 1). Similar differences between X-ray and SEM results were noted in previous studies of the CaO–Al_2O_3 system [1], and to a lesser extent in the MgO–Al_2O_3 system [2]. In the present experiments, comprehensive current/time data were recorded, providing an opportunity to examine this question by independent calculations based on Faraday's laws. Since the quantity, Q, of material transferred by electrolysis is related to the current, I, flowing for time, t, the equivalent weight, W, and the valency, n, of the transferred species by

$$Q = ItW/(nF), \quad (4)$$

where F is the Faraday ($\approx 96\,500$ C), the amount of Ca^{2+} electrolysed into the silica pellets can be estimated from the integrated area under the current/time plots which corresponds to (It), the total charge transferred. Fig. 6 shows current/time plots for the SiO_2(− ve) experiments at the two lowest temperatures; this polarity was used in the calculations since it corresponds to the movement of solely Ca^{2+} into silica, without the complication of Si counter-migration.

Fig. 6 shows an initial steep drop in the current density due to the rapid depletion of mobile charge carriers (probably monovalent impurity ions) followed by a more gradual continuous change for the duration of the experiment. The SiO_2(+ ve) curves, not shown in Fig. 6, have slightly different characteristics, reaching an almost steady state early in the experiment; the current densities were also greater in the SiO_2(+ ve) experiment than in the corresponding SiO_2(− ve) experiments.

Substitution into Equation 4 of the (It) values derived from Fig. 6 by measuring the area under the curves shows that the electrolysis experiment at 1250° C resulted in the transfer of 6.19 mg Ca^{2+}, while at 1300° C, 9.03 mg Ca^{2+} was transferred. Assuming that all of this Ca forms calcium silicates in the interfacial region, the Ca^{2+} transferred at 1250° C corresponds to 17.95 mg CS or 13.31 mg C_2S formed, which in turn corresponds to a thickness of 111 μm of CS or 74 μm of C_2S (assuming densities of 2.92 and 3.28 g cm^{-3} for

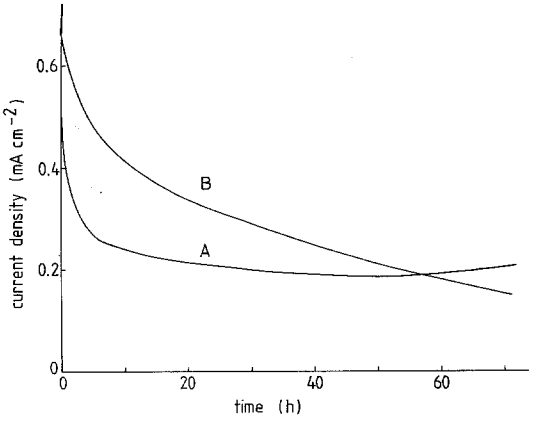

Figure 6 Relationship between current density and time for electrolysed CaO/SiO_2 couples, SiO_2 negative. Curve A, 1250° C, Curve B, 1300° C.

α-CS and β-C_2S, respectively). At 1300° C, 26.19 mg CS or 19.41 mg C_2S would be formed, having a thickness of 151 and 100 μm, respectively. If allowance is made for the fact that the silica host matrix is only 88% dense, these thicknesses are slightly increased (126 and 84 μm at 1250° C and 172 and 114 μm at 1300° C). The reaction product thicknesses thus calculated represent limiting cases, since the reaction zones of the SiO_2 (−ve) samples contain both CS and C_2S; the predominance of CS noted in all samples suggests, however, that the bias should be towards the larger calculated thicknesses. These results are in excellent agreement with the X-ray measurements, and suggest that the EDAX measurements are consistently under-estimating the penetration distance. Possible reasons may lie in the much smaller analysis area of EDAX compared with X-ray, coupled perhaps with a diluting effect of the silica host matrix and the consequent difficulty of detecting small Ca concentrations in a high Si background. Since this effect is consistent throughout all the SEM measurements, the diffusion activation energies derived from the EDAX profiles should be unaffected, and although the absolute values of ln D could be in error by up to 12% because of the error of the penetration distance, this precision is no worse than might have been expected, in view of the other difficulties associated with these measurements.

3.3. Effective electrical mobility of the migrating species

In a study of the $MgO-Al_2O_3$ system [2], elemental concentration profiles of the electrolysed and unelectrolysed samples were used to estimate values of Δ, the downfield shift of the diffusion profile in the electric field, E, from which the effective electrical mobility of the migrating species (μ_{eff}) is derived from:

$$\mu_{eff} = \Delta/Et, \quad (5)$$

where t is the reaction time. In similarly analysing the present results, the field-hindered profile was used, since (i) the downfield shifts of this profile, although negative in sign, are larger than the field-assisted downfield shifts and therefore less susceptible to measurement error; and (ii) the electric field attained a steady state early in the field-hindered experiments, making a mean value of E easier to estimate. Although, as shown in the previous section, the element concentration profiles probably consistently underestimate the true penetration distance, the present measurements, involving *differences* between the various profiles, should not be too adversely affected. Furthermore, the co-existence of various silicate phases, each with its own profile, militates against the use of X-ray measurements to estimate mean downfield shifts.

Table I shows the values of μ_{eff} derived from Equation 5 for the three lowest temperatures. Measurements were not made on the 1400° C profile because of difficulties in establishing the position of the original interface in these experiments (see Section 3.1.).

For comparison purposes, values of μ_{eff} were also estimated from:

$$\mu_{eff} = \mu(\sigma_0/\sigma), \quad (6)$$

where μ is the true mobility of the migrating species and σ_0 and σ are the electrical conductivities of the pure oxide and product phase, respectively. As in the previous work [2], μ was derived from the self-diffusion coefficient of the migrating species in its oxide using the Nernst–Einstein relationship, the values of D being taken from the data of Lindner for sintered polycrystalline CaO annealed in air [10]. Since the results of Section 3.1 suggest that the process

TABLE I Effective electrical mobilities of Ca in the $CaO-SiO_2$ system, estimated both from diffusional shift distances Δ and calculated from conductance and diffusion data by Equation 6. Diffusion time $t = 2.592 \times 10^5$ sec, mean field strength $E = 1.69 \times 10^3$ V cm^{-1}

Temperature (° C)	Δ ($\times 10^{-5}$ cm)	μ_{eff} (from Equation 5) ($\times 10^{-12}$ cm^2 sec^{-1} V^{-1})	σ_0/σ	μ_{eff} (from Equation 6) ($\times 10^{-12}$ cm^2 sec^{-1} V^{-1})	
				(a)	(b)
1250	0.57	1.30	0.23	3.32	4.32
1300	0.95	2.17	0.17	5.39	7.06
1350	2.03	4.64	0.16	10.90	13.90

Note: Mobilities in column (a) derived from diffusion data for Ca in CaO [10], mobilities in column (b) from data for Ca in β-CS [10].

might be controlled by Ca migration through the interfacial calcium silicates, values of μ were also calculated from such data as were available for Ca diffusion in relevant silicate phases (α-CS, β-CS, α'-C_2S) [10].

The electrical conductivities for substitution in Equation 6 were taken from data for polycrystalline pellets of CaO and β-C_2S in air [12]. These values were used in preference to other published data since they were obtained for similar samples and under similar conditions to the present electrolysis experiments. Although electrical conductivity data for CS may have been preferable to β-C_2S, since the former phase occurred more universally in all the samples, suitable CS data were not available. The values of μ_{eff} calculated from Equation 6 are shown in Table I, which includes calculations based on the diffusion of Ca in both CaO and β-CS. Several points emerge from Table I:

(i) as in previous work [1, 2], the effective mobilities derived by the two methods agree within an order of magnitude, but, contrary to both previous studies, the value derived from Δ is *smaller* than those calculated from electric conductances;

(ii) the mobilities calculated from Equation 6 using diffusion data for Ca in CaO (column a) and in β-CS (column b) are in equally good agreement with the downfield shift values (although the mobilities derived from diffusion data for the other silicate phases are not shown in Table I, they are generally within an order of magnitude of the downfield shift values;

(iii) the effective mobilities derived from Ca in CaO (column a) are consistently larger than the values derived from Δ by a factor of ~ 2.4, while the data for Ca in β-CS yield mobilities consistently larger by a factor of ~ 3.2.

These results confirm previous suggestions that effective mobilities calculated from Equation 6 provide an order-of-magnitude value only [2], and furthermore, suggest that differences between mobilities derived from Equations 5 and 6, although consistent within a particular system, are not necessarily the same for other systems, particularly of different valency combinations. Whether the similarities previously observed in $CaO-Al_2O_3$ and $MgO-Al_2O_3$ [1, 2] are real or fortuitous is still unclear, and the elucidation of any systematic relationship awaits further work on other oxide combinations.

4. Conclusions

(1) The application of d.c. electric fields to polycrystalline $CaO-SiO_2$ diffusion couples slightly enhances the diffusion of Ca into the silica when the latter is negatively charged, and markedly hinders the diffusion when the polarity is reversed. Analysis of the Ca penetration data is difficult for the higher temperature experiments (1350 and 1400° C) because of the formation of a loose, powdery interfacial band of γ-C_2S reaction product on cooling the sample, but if allowance is made for this by weighing, the diffusion coefficients for the SiO_2(− ve) experiments are similar to those of the unelectrolysed samples, and have activation energies similar to that reported for Ca diffusion in α-CS [10]. A much larger activation energy is found for Ca diffusion in the field-hindered experiments.

(2) The crystalline silicate interfacial products in the SiO_2(− ve) experiments include β-C_2S, possibly stabilized by excess Ca which also appears as interfacial CaO in these experiments. Under all conditions, α-CS is a major reaction product, and is the sole silicate present in the SiO_2(+ ve) samples, which also contain interfacial tridymite, possibly stabilized by the electrolysis of Na^+ and K^+ impurities from the silica into the interfacial region.

(3) Significant differences exist between the degree of Ca penetration measured by EDAX and X-ray methods. Faraday's law calculations of product thickness based on the amount of Ca^{2+} transported suggest that the X-ray measurements are more realistic.

(4) Calculations of the effective electrical mobility of Ca in the $CaO-SiO_2$ system derived from electrical conductivity and diffusion data agree within an order of magnitude with values derived from downfield shift measurements of the diffusion profile.

Acknowledgements

We are indebted to Mr W. Kitt for the flame photometry of the silica materials, and to Mr G. D. Walker for the SEM/EDAX analyses.

References

1. K. J. D. MACKENZIE and R. K. BANERJEE, *J. Mater. Sci.* **14** (1979) 339.
2. K. J. D. MACKENZIE and M. J. RYAN, *ibid.* **16** (1981) 579.
3. J. GEBAUER and E. FITZER, *Zement-Kalk-Gips* **58** (1969) 402.

4. R. HAYAMI and T. OGURA, *Osaka Kogyo Gijutsu Shikenjo Kiho* **20** (1969) 270.
5. E. K. BELYAEV, *Isves. Akad Nauk SSSR, Neorg. Mater.* **13** (1977) 2031.
6. W. JANDER and E. HOFFMANN, *Z. Anorg. Allgem. Chem.* **218** (1934) 211.
7. H. F. W. TAYLOR, "The Chemistry of Cements", Vol. 2 (Academic Press, London, 1964) p. 359 ff.
8. G. BREBEC, R. SEGUIN, C. SELLA, J. BEVENOT and J. C. MARTIN, *Acta Metall.* **28** (1980) 327.
9. P. KOFSTAD, "Nonstoichiometry, Diffusion and Electrical Conducticity in Binary Metal Oxides" (Wiley-Interscience, New York, 1972) p. 129.
10. R. LINDNER, *J. Chem. Phys.* **23** (1955) 410.
11. S. N. GHOSH, P. B. RAO, A. K. PAUL and K. RAINA, *J. Mater. Sci.* **14** (1979) 1554.
12. K. J. D. MACKENZIE, *Trans. J. Brit. Ceram. Soc.* 77 (1978) 13.

Received 30 March
and accepted 2 July 1982